



Steric effects of trialkyl phosphates on the extraction of uranyl cation

Rupa Shantamal Madyal, Vilas Gajanan Gaikar*

Department of Chemical Engineering, Institute of Chemical Technology, Matunga, Mumbai 400 019, India
Tel. +91 22 3361 2013; Fax: +91 22 33611020; email: vg.gaikar@ictmumbai.edu.in; v.g.gaikar@gmail.com

Received 9 December 2010; Accepted 13 September 2011

ABSTRACT

We report gas phase calculations on uranyl ions (UO_2^{2+}) complexes with symmetrical trialkyl phosphates, $(\text{RO})_3\text{PO}$, as ligand (L), where, R is a linear or branched propyl, butyl and amyl groups. Density functional theory (DFT) using double numerical polarization (DNP) basis set with restricted scalar relativistic effect is used to validate the structural features of $\text{UO}_2(\text{NO}_3)_2\text{L}_2$ complexes against experimental XRD data. The interaction energy and extraction ability of the trialkyl phosphates are compared for uranyl (VI) ion. Steric effect of the extracting agent that governs the metal extraction is explained in terms of cone angles made by ligands towards metal ion. The complexation behaviour of straight chain and branched chain ligands is well understood by this study. The relative order of cone angles and interaction energies from DFT simulation follow the trend with the experimentally determined distribution coefficients. An interesting approach of this work is the importance of cone angle in the solvent extraction.

Keywords: Steric effect; Uranyl(VI) ions; Cone angle; Trialkyl phosphates; Density functional theory; Molecular modeling; Interaction energy; Partition coefficient

1. Introduction

In nuclear power generation, separation of U and Pu from other fission products and from each other in irradiated fuel by solvent extraction is one of the challenging tasks. Tri-*n*-butyl phosphate (TBP) is the most widely used extractant in dodecane as a diluent. Several phosphorus based extractants, such as phosphates, phosphinates, phosphonates and phosphine oxides, have been extensively studied to understand the role of the extractant's structure on its extraction efficiency [1–4]. Yet, we lag in deciphering the role of the ligand structure in its extraction efficiency for a particular metal ion. The study of ligands with metal ions in terms of their structures, interactions and energetics using Molecular Modeling can provide useful and necessary information

for their applications and can reduce expensive and hazardous experimentation.

The most comprehensive work by molecular mechanics (MM) calculations has been presented by Sella and Bauer in a series of papers that showed the importance of association and electrostatic energy in extraction efficacy of the ligands for the metal ions [5–7]. Rabbe et al. have reported a regression model based on charge parameters (sum of atomic charges of amidic functions of monoamides) and association energy calculated from molecular orbital approach for correlating $\log D_{\text{U(VI)}}$ [8]. Varnek et al. have performed quantitative structure–property relationship (QSPR) modeling (based on fragment descriptors) of the distribution coefficient of uranyl extracted by phosphoryl-containing podands [9]. Gas phase studies reported so far discuss extractability of U(VI) with neutral organophosphorus agents such as, trimethyl phosphate, triethyl phosphate

*Corresponding author.

and TBP [10,11]. These studies mainly dealt with bond overlap population obtained from discrete-variational Dirac–Slater (DV-DS) molecular orbital method to elucidate the variation in extractability without considering different conformations of the ligands.

Many efforts have been devoted to empirically correlate extraction properties of the ligands with their physico-chemical parameters [12–16]. For instance, Shi and McCullough have studied 314 metal cation–solvent–ligand combinations using MM, molecular dynamics (MD) and multiple linear regressions to correlate molecular descriptors such as radius and electronegativity of metal cations, dielectric constant of solvents, energy components and total energy of the ligands [12]. Experimental data on the extraction of actinide elements by phosphoryl-containing ionophores also have been correlated with other descriptors such as group electronegativities or Taft parameters of molecular fragments, atomic charges, energies of 1s-orbitals of oxygen atoms, electrostatic potential distribution, chemical softness and donor–acceptor interaction energies [13–15]. To assess the relative extractability of trivalent lanthanide cations coordinated to organophosphate and aqua ligands, Comba et al. used the strain energy difference calculated by MM between lanthanoid cations and La(III) to relate their extractability [16].

The extraction of actinides with trialkyl phosphates is still poorly understood and there are no reported theoretical studies on the structural effects of trialkyl phosphates on their distribution coefficients. Therefore, we considered the linear and branched chain trialkyl phosphate ligands for the simulation. The experimental distribution coefficient data of U(VI) have been reported by Nomura and Hata [2] using 0.732 M solutions of trialkyl phosphates in carbon tetrachloride, and by Siddall [1] and Suresh et al. [3] and Rao et al. [4] using 1.09–1.1 M solutions in *n*-dodecane with 3 M nitric acid. These experimental data were taken for comparison with the simulated results.

The investigation of complex structures of known ligands with metal ions and predicting those of unknown ligands by molecular simulation is one of the efforts to design newer and possibly more effective ligands. This requires a systematic study of intrinsic interactions between the metal and the extractant. The present work, therefore, is devoted to determine stable structures of $\text{UO}_2(\text{NO}_3)_2\text{L}_2$ where L = TPP (tripropyl phosphate), TBP, TiBP (tri-isobutyl phosphate), TsBP (tri-secbutyl phosphate) and TAP (tri-*n*-amyl phosphate) and to estimate binding interactions amongst these complexes in the gas phase by density functional theory (DFT) calculations.

The work is performed in three steps: First, the theoretical methodology is validated using the molecule/complex for which enough experimental information is

available. The crystal structures of organophosphate-U(VI) complexes, available in literature, of $\text{UO}_2(\text{NO}_3)_2(\text{TBP})_2$ and $\text{UO}_2(\text{NO}_3)_2(\text{TiBP})_2$ are used for validation [17,18]. Second, the structural properties of $\text{UO}_2(\text{NO}_3)_2(\text{TPP})_2$, $\text{UO}_2(\text{NO}_3)_2(\text{TsBP})_2$ and $\text{UO}_2(\text{NO}_3)_2(\text{TAP})_2$ complexes are studied theoretically and third, the simulated characteristics of the systems are correlated with the extraction ability of the ligands.

2. Computational methods

The ligands and uranyl cation were constructed using Materials Studio (MS) (*ver* 4.1, Accelrys Inc., USA). MM calculations were performed in the FORCITE module of MS using universal force-field (UFF) which is a purely diagonal and harmonic force-field [19]. In UFF, the bond stretching is described by a harmonic term, angle bending by a three-term Fourier cosine expansion, and torsions and inversions by cosine-Fourier expansion terms. The van der Waals interactions are described by the Lennard-Jones 12-6 potential. The electrostatic interactions are described by atomic monopoles and a screened (distance-dependent) Coulombic term. The UFF includes a parameter generator that calculates the force-field parameters by combining the atomic parameters. The partial charges on ligands and uranyl ion were calculated using QEq method, based on the equilibration of atomic electrostatic potentials with respect to a local charge distribution [20]. We pre-optimized all structures by MM to reduce computational effort of the complete optimization by DFT.

The conformational search was performed on metal free ligands by Conformers Simulation module of MS. The search was done using a systematic grid scan method which varies one or more specific torsion angles over a grid of equally spaced values. If more than one torsion angle is varied, all the possible combinations are explored. The Filter tab option of the module was selected for filtering out high energy conformers, i.e., conformers with absolute energy more than 100 kcal/mol, which are unlikely to be significant. Thus, reasonable sampling of the low energy conformations, i.e., structures with energy lower than 100 kcal/mol, are retained. The accepted conformers were taken for the minimization again, and finally these optimized structures were filtered for the second time and then stored. The selected conformers were used to build 1:1 complexes of L: UO_2^{2+} in the absence of other competing environments and then subjected to the DFT calculations for stability considerations.

The optimized structures from the MM calculations were further re-optimized using DFT until a final convergence threshold for the maximum energy change of 0.00001 Ha, i.e., 0.006 kcal/mol, was obtained. Due to inclusion of electron correlation and relativistic effects, this approach has proven to be useful to predict

accurate geometries at a much less computational cost. All the complexes have been fully optimized using generalized gradient density approximation (GGA) without imposing any symmetry in the present calculations [21]. Though, hybrid B3LYP functionals is recommended for heavy metal ions [22], we used BLYP functional [23,24] because of non-availability of B3LYP in MS and it provides results closer to the results with B3LYP [22]. We performed the calculations using restricted scalar relativistic all-electron method based on Douglas and Kroll [25] and Koelling approach [26]. The double numerical basis set which includes all electrons plus polarization functions (DNP), comparable to 6-31G** was used by means of DMol³ module of MS.

3. Results and discussion

Before we discuss results for fully optimized uranyl complexes with various trialkyl phosphates, we need to consider different conformation(s) of a ligand to investigate the influence of the ligand conformation on its complexation with a metal ion.

3.1. Uncomplexed ligands

The ligands were built with different O=P–O–C torsional angles to predict the suitable conformation. To find a stable conformer in the presence of metal ion and to reduce computational time, TPP and TBP were considered as excellent candidates. The optimized conformers of free TBP in a simplified form are displayed in Fig. 1, schematically as *trans* ($t \sim 180^\circ$) and *gauche*

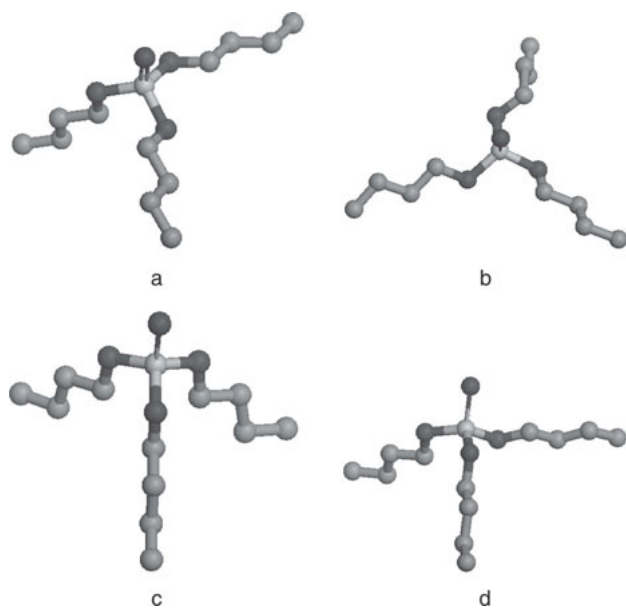
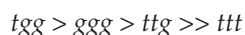


Fig. 1. Conformations of TBP with different O=P=O–C torsion angles (a) *tgg* (b) *ggg* (c) *ttt* and (d) *ttg* (hydrogen atoms are not shown for clarity).

($g \sim 60^\circ$). The real situation for the ligand population is in solution and the preferred conformer in gas phase and in solution could be different. Earlier MD studies had shown that the *ggg* conformer of TBP transforms into the *tgg* conformer in the uncomplexed form in the aqueous as well as chloroform solutions which indicates that population of *tgg* conformer could be larger in solution [27]. However, a stable conformer in an uncomplexed state may not be preferred in the complexed state and therefore, all conformers of TBP and TPP were used as starting structures to build the 1:1 complex with uranyl cation. In both the cases, the *tgg* conformer was found to be the most suitable conformer for complexation. For the *ttt* and *ttg* conformers of TPP as well as those of TBP, the total energy was calculated as single point energy as these conformers transform into respective *tgg* conformer during optimization. The following stability order is found in vacuo for uncomplexed TBP conformers:



The uncomplexed *ggg* conformer is stable by 1.0 kcal than the *tgg* conformer. The *ttt* conformer is of the highest energy amongst the conformations, being some 133.9 kcal/mol less stable than the *tgg* conformer. The *ttg* conformation lies 107.5 kcal/mol above the *tgg* conformer but it is 25.4 kcal/mol below the *ttt* conformer in energy. These results are consistent with *ab initio* calculations on $\text{O}=\text{P}(\text{OCH}_3)_3$, which find that the *tgg* and *ggg* conformers are the most stable ones [28]. The *ttt* and *ttg* conformers having two and three *trans* dihedral angles, respectively, suffer from hydrogen–hydrogen repulsion and, therefore, it is highly unstable among the conformers. The similar trend is observed for two conformers of TPP. The *ggg* conformer is lying 0.98 kcal/mol below in energy than the *tgg* conformer. (Electronic energy and relative energies of the conformers are given in supporting information Table S2.)

3.2. The $\text{L}:\text{UO}_2^{2+}$ complexes

The interaction energy (IE) as ΔE between the uranyl ion and the ligand with its different forms was calculated by subtracting the summation of the energies of the metal ion and the metal free ligand from that of their 1:1 complex. The IE values between the ligand and the uranyl cation, UO_2^{2+} were calculated as $\Delta E = \text{TE}_{\text{complex}} - \text{TE}_{\text{ligand}} - \text{TE}_{\text{uranyl cation}}$ and are given in Table 1. According to these calculations, ΔE between *tgg* conformer of TPP and uranyl ion (1:1 complexes), showed better stability by 2 and 12 kcal/mol, with respect to its *ggg* and *ttt* conformers, respectively.

Table 1
The optimized geometries for organophosphorous uranyl nitrate complexes with experimental values and MS results

Complex	Method	U-O (Å)	U-O(N) (Å)	U-L (Å)	U-O-P (degree)
$\text{UO}_2(\text{NO}_3)_2\text{TiBP}_2$	EXAFS ^a	1.78	2.53	2.37	156.3
	X-ray ^b	1.76	2.51	2.37	164.3
	EXAFS ^a	1.78	2.54	2.38	157.3
	DMol ³	1.81	2.57	2.50	157.7
$\text{UO}_2(\text{NO}_3)_2\text{TBP}_2$	EXAFS ^a	1.78	2.54	2.41	172.1
	DMol ³	1.81	2.58	2.50	174.6
$\text{UO}_2(\text{NO}_3)_2\text{TPP}_2$	DMol ³	1.82	2.58	2.49	176.4
$\text{UO}_2(\text{NO}_3)_2\text{TsBP}_2$	DMol ³	1.82	2.58	2.49	166.5
$\text{UO}_2(\text{NO}_3)_2\text{TAP}_2$	DMol ³	1.82	2.58	2.51	173.1

^aRef. [17].

^bRef. [18].

Similar studies of TBP conformers, however, showed that *tgg* conformer is stable than the *ttg* conformer by a very large energy, i.e., 83 kcal/mol. For the *ttt* conformer of TPP as well as that of TBP, the total energy of the complex was calculated as single point energy as this conformer get transformed into *tgg* conformer during optimization. Fully relaxed structure of $\text{L}:\text{UO}_2^{2+}$ with different conformers when subjected to geometry optimization with all degrees of freedom, yielded final structure as *tgg* conformer. This shows that during complexation ligand changes its conformation. This transformation suggests the following observations: First, coordination of a uranyl ion to a ligand may change the conformation of the ligand. Second, *tgg* conformer is the predominant form of the ligand for the complexation as far as TBP and TPP are concerned. Among the LUO_2^{2+} complexes with neutral ligands, ΔE decreases in the order *tgg* > *ggg* > *ttg* > *ttt*. These results are consistent with quantum mechanical calculations on $\text{M}^{3+}:\text{O}=\text{PR}_3$ (where $\text{M}^{3+} = \text{La}, \text{Eu}, \text{Yb}$) complexes [29]. Optimization of complexes of UO_2^{2+} with low-lying L conformers was performed and the relative energies and interaction energies is shown in Table S4. This is why the *tgg* conformer of each trialkyl phosphates was selected to construct the $\text{UO}_2(\text{NO}_3)_2\text{L}_2$ complexes (Fig. 2).

3.3. Comparison with experimental structures

It is a well known fact from experiment [17,18] and molecular simulation [11] studies, that the molecular structure of the uranyl(VI) nitrate complex has a hexagonal bipyramidal structure with eight donor atoms around the central U atom, two bidentate nitrate groups and two monodentate phosphate ligands in *trans* position within $\text{O}=\text{U}=\text{O}$ equatorial plane. The optimized TBP complex is in agreement with these results as

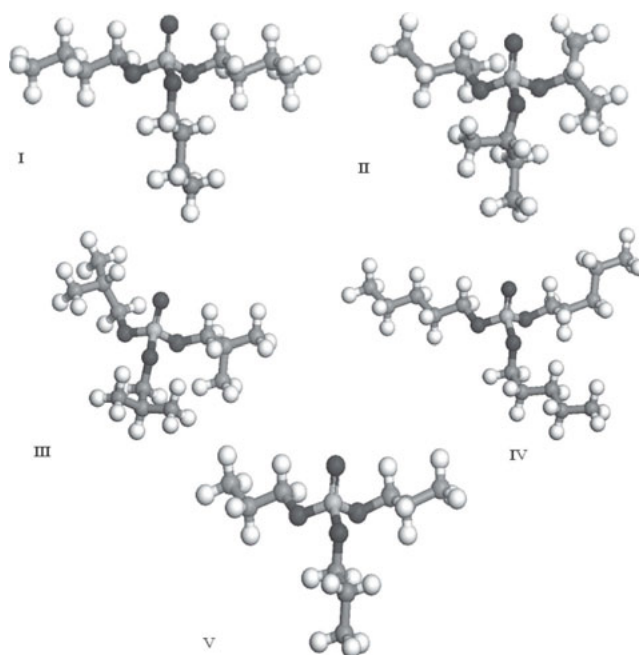


Fig. 2. Optimized structures of trialkyl phosphates (a) TBP (b) TsBP (c) TiBP (d) TAP and (e) TPP.

shown in Fig. 3. The simulated structure is further supported by the XRD data. The optimized geometries of the $\text{UO}_2(\text{NO}_3)_2\text{L}_2$ complexes are compared with the experimental data in Table 1. The difference between experimental and calculated bond distances is denoted by Δ . The calculated distances of U–L ($\Delta = +0.13$ Å with TiBP and $\Delta = +0.09$ Å with TBP) and U–O distances ($\Delta = 0.03$ – 0.05) are in close agreement with the results of X-ray diffraction and EXAFS experiments [17,18]. The U–L distances are, however, overestimated by ~ 0.1 Å, due to either the BLYP functional (reported to

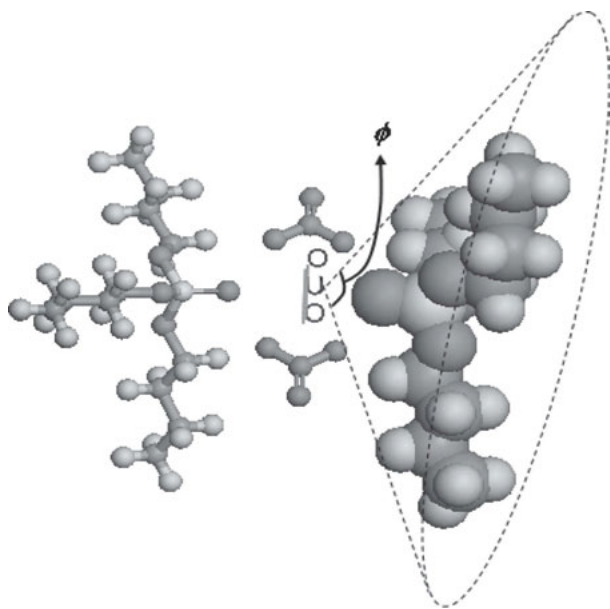


Fig. 3. Optimized geometry of $\text{UO}_2(\text{NO}_3)_2\text{TBP}_2$ complex with cone angle ϕ .

give overestimated bond lengths [22,30]) or neglect of the solvation effect in the present studies and has been now a part of our further and continuing investigations. The results indicate that uranyl phosphate complexes have the same geometry in the solid-state as in the gas phase. A comparison of experimental [17,18] and calculated structures obtained by DMol³ thus, reveals an expected degree of agreement: bond angles within $\pm 2.5^\circ$ and bond lengths within $\pm 0.1 \text{ \AA}$. Qualitatively, we note that the DFT calculations reproduce the experimentally observed structures. The effect of the ligand structure on the extractability of the metal ions, however, is not clear from this information.

3.4. The $\text{UO}_2(\text{NO}_3)_2\text{L}_2$ complexes

The interaction energy between the ligand and the salt $\text{UO}_2(\text{NO}_3)_2$ was calculated as $\Delta E = \text{TE}_{\text{complex}} - \text{TE}_{\text{ligand}} - \text{TE}_{\text{salt}}$ in the $\text{UO}_2(\text{NO}_3)_2\text{L}_2$ complexes using all corresponding optimized geometries. Here, TE means total energy of complex or molecule.

The ΔE in $\text{L}_2\text{UO}_2(\text{NO}_3)_2$ drops markedly (by about a factor 4), compared to ΔE in the charged LUO_2^{2+} complexes. This is due to a change in the electrostatic interactions which are mostly of a charge–dipole type in LUO_2^{2+} complexes (179–283 kcal/mol) and of a dipole–dipole type in the $\text{L}_2\text{UO}_2(\text{NO}_3)_2$ (–46 to –57 kcal/mol). The metal–ligand interactions are softer in $\text{L}_2\text{UO}_2(\text{NO}_3)_2$ than in LUO_2^{2+} complexes. Amongst TBP isomers, the TsBP complex is stable by 0.83 and 0.69 kcal/mol than TiBP and TBP, respectively.

The addition of counter-ions to the metal ion leads to marked drop in ΔE , by a factor of four with TBP and TPP. In the $\text{L}_2\text{UO}_2(\text{NO}_3)_2$ complexes with neutral monodentate ligands, none yields a ΔE interaction as strong as the TsBP ligand.

The addition of counter-ions to LUO_2^{2+} complexes leads to a drop of the ΔE values, and a lengthening of the metal ligand bond distances. In the charged complexes on an average the ligand metal bond distances are 2.37 Å and in neutral complexes 2.47 Å.

The simulation results suggest that the ligand is largely responsible for the interaction energy of the system. These energies range from –46 to –57 kcal/mol and are dependent on the ligand structure. The IE is also strongly related to the distribution coefficient of the complex as shown in Fig. 4. However, the changes in ΔE with a given ligand are much smaller as compared to changes in K_d . The K_d values reported by Nomura et al. [2] are slightly higher than those reported by Siddall [1] but follow the same trend. Whereas, Suresh et al. [3] and Rao et al. [4] reported much lower values than the above two groups with almost constant K_d . The discrepancy in the experimental K_d values reported by different groups indicates a need for more accurate experimental studies.

3.5. Cone angles

An interesting aspect of the complexation is wrapping around the cation by a ligand to prevent the binding of water molecules with the cation. The coordination of the cation by solvent molecules may significantly perturb intrinsic binding features. Increase in binding efficiency and selectivity can be obtained when the ligand molecules wrap sufficiently around metal ion. Wrapping of ligands can be calculated with the help of cone angles made by ligands towards the metal ion.

To estimate the cone angle made by the complexing ligands with the central metal ion, the ligands from the DFT optimized complexes were built with CPK model and the cones were created from U atom as an apex around the ligand molecules as shown in Fig. 3. The cone angle increases with the increase in carbon chain length and with branching in the alkyl chain near the phosphoryl group. In linear alkyl phosphates, the cone angle increased from 89° to 117° , i.e., from TPP to TAP. However, among the TBP isomers, the cone angle is largely increased from *n*-TBP to *sec*-TBP, i.e., from 110° to 124° . It is obvious that the branched ligands make a greater cone angle with the metal ion as compared to straight chain ligands. It should be noted that they also show a correlation with the experimental distribution coefficients, i.e., a well protected metal ion by the ligand will have better distribution towards the organic phase.

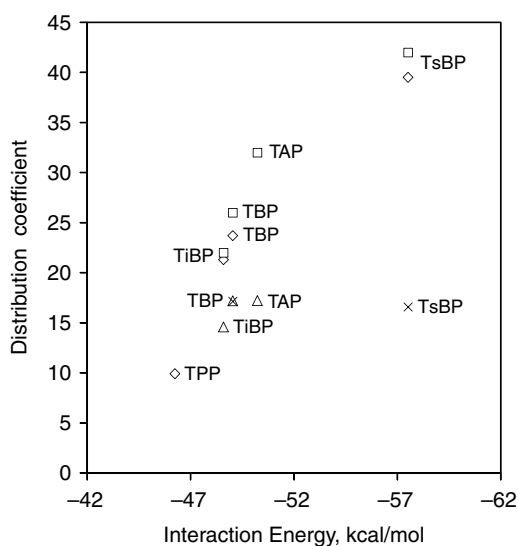


Fig. 4. Interaction energy vs distribution coefficient. \diamond – Ref. [2], \square – Ref. [1], Δ – Ref. [3] and \times – Ref. [4].

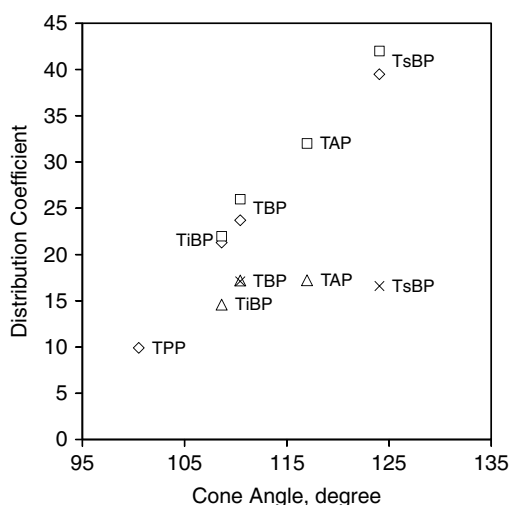


Fig. 5. Cone angle vs distribution coefficient. \diamond – Ref. [2], \square – Ref. [1], Δ – [3] and \times – Ref. [4].

A plot of distribution coefficient (K_d) versus cone angle is shown in Fig. 5. This plot reveals a distinct correlation between the cone angle and the efficacy of a ligand in the extraction of uranyl ion. Importantly, this approach shows better insight into the extraction mechanism and one of the theoretical ways toward engineering an efficient ligand for the extraction.

Generally, steric attributes of the ligands are quantified in terms of cone angles [31,32]. Greater is the cone angle made by a ligand, better is the wrapping of the cation and lesser is the dissociation of complex.

This could be contrary to the approach that sterically demanding ligands facilitate the dissociation of the complex. The latter is possible if cone angle is too large to retain the geometry of the complex. In other words, steric crowding can destabilize the complex after a certain cone angle. To remove the binding counterions from the first coordination sphere, the cone angle of ligand should be 180° . This indicates that, in absence of the counter-ions, ligand effectively protects one half of the coordination sphere of the metal complex. In the present calculations, considering bidentate nitrate ions and monodentate ligands in the first coordination sphere, the cone angle is less than 180° . In that case, question of steric hindrance does not arise and dissociation of the complex is indisposed.

4. Conclusions

Molecular simulation can be used as a complementary tool to determine geometric parameters of heavy metal complexes for which experimental data are not available. In this paper, we have successfully investigated molecular structures of TPP, TsBP and TAP complexes for their geometries which are not yet established experimentally. It is apparent from the correlation that cone angle is a reliable parameter to design a new ligand for effective extraction of a metal ion. The simulation agrees with the experimental work that the extraction ability increases with the size of ligand and branching within the alkyl group. The contribution of cone angle is significant in deciphering the alkyl substituent effect on the complexation with a metal ion. Thus, analysis of the results points to a better extractability by TsBP and TAP among the selected organo-phosphorus series.

Our theoretical study has provided cone angle as a new parameter that correlates well with the experimental distribution coefficient and such an approach is valuable in the design of ligand with high specificity and can be extended to other complex molecular processes. A systematic detailed study with the solvent effect will be the part of further communications.

4.1. Supporting information available

Table S1 provides energetics of $\text{UO}_2(\text{NO}_3)_2 \cdot \text{L}_2$ complexes. Table S2 provides energetic of various uncomplexes and complexed ($\text{UO}_2^{2+} \cdot \text{L}$) conformers. Table S3 provides relative energies of TPP and TBP conformers, Table S4 gives Electronic and interaction energies of low lying conformer of ligands (*tgg*) with UO_2^{2+} cation. Also are given co-ordinates of the optimized structures.

Supporting information

Table S1
Energetics of $\text{UO}_2(\text{NO}_3)_2 \text{L}_2$ complexes

	Total electronic energy (a.u.)	Interaction energy, (kcal/mol)
TPP	-32421.349444	-46.239
TBP	-32657.347274	-49.037
TiBP	-32657.346109	-48.587
TsBP	-32657.362988	-57.511
TAP	-32893.340179	-50.225

Table S2
Total and relative energies of TPP and TBP conformers

Conformers	Total electronic energy (a.u.)		Relative energy (kcal/mol)	
	TPP	TBP	TPP	TBP
<i>ggg</i>	-999.593169	-1117.589817	0.00	0.00
<i>tgg</i>	-999.591604	-1117.588180	0.98	1.03
<i>ttg</i>	-999.414676	-1117.416860	112.00	108.53
<i>ttt</i>	-999.378956	-1117.376379	134.42	133.93

Table S3
Total and relative energies of TPP and TBP conformers with UO_2^{2+} cation

Conformers	Relative energy (kcal/mol)		Interaction energy (kcal/mol)	
	TPP	TBP	TPP	TBP
<i>ggg</i>	1.59	3.03	-168.86	-176.31
<i>tgg</i>	0.00	0.00	-171.42	-180.36
<i>ttg</i>	1.38	242.43	-281.06	-45.43
<i>ttt</i>	126.04	268.49	-178.82	-44.78

Table S4
Electronic and interaction energies of low lying conformer of ligands (*tgg*) with UO_2^{2+} cation

Ligands	Electronic energy (a.u.)	Interaction energy (kcal/mol)
TPP	-30859.144349	-168.86
TBP	-30977.155172	-180.35
TiBP	-30977.147390	-182.17
TsBP	-30977.141428	-173.36
TAP	-31095.163036	-188.12

Coordinates of complexes

1. $\text{UO}_2(\text{NO}_3)_2 \text{TBP}_2$				O	4.4226	4.4674	6.3885
C	-8.5328	6.9896	4.0412	C	4.4389	-0.5002	6.9654
C	-7.5841	6.9768	2.8277	C	4.0722	0.6727	6.0366
C	-6.0997	6.8652	3.2356	C	4.4524	2.0465	6.6302
C	-5.1659	6.8524	2.0299	C	4.0995	3.1913	5.6883
P	-2.5279	6.4935	1.5879	O	4.4746	6.9494	6.8041
O	-1.2713	6.4818	2.3991	C	5.8866	10.7203	8.6606
O	-3.7788	6.7554	2.5429	C	5.9008	9.4428	7.8013
O	-2.7715	5.1322	0.7621	C	5.5632	8.1731	8.6077
C	-2.7729	0.1984	-0.0935	C	5.5774	6.8830	7.7943
C	-2.3860	1.3228	0.8857	H	8.3890	7.8675	-0.1510
C	-2.7709	2.7266	0.3693	H	7.5996	6.2807	-0.0573
C	-2.3746	3.8211	1.3530	H	9.0416	6.6147	0.9237
O	-2.6657	7.6197	0.4671	H	6.3082	8.0249	1.2480
C	-1.3986	10.4255	-3.4747	H	7.7406	8.3735	2.2134
C	-1.0384	9.1954	-2.6205	H	7.7145	6.0206	3.1225
C	-2.0302	8.9671	-1.4592	H	6.2917	5.6531	2.1355
C	-1.6560	7.7474	-0.6257	H	6.3886	7.7928	4.3422
H	-8.3194	7.8404	4.7030	H	4.9526	7.3531	3.3690
H	-8.4290	6.0703	4.6346	H	4.1432	-1.4604	6.5222
H	-9.5810	7.0672	3.7228	H	3.9322	-0.4085	7.9364
H	-7.7349	7.8938	2.2363	H	5.5211	-0.5340	7.1545
H	-7.8480	6.1358	2.1674	H	4.5750	0.5388	5.0659
H	-5.9391	5.9473	3.8194	H	2.9917	0.6535	5.8318
H	-5.8238	7.7069	3.8862	H	3.9248	2.1983	7.5828
H	-5.3567	5.9932	1.3755	H	5.5300	2.0751	6.8487
H	-5.2409	7.7759	1.4442	H	3.0317	3.2135	5.4536
H	-2.2783	0.3320	-1.0660	H	4.6881	3.1512	4.7644
H	-3.8576	0.1805	-0.2702	H	6.1283	11.6045	8.0555
H	-2.4797	-0.7839	0.3003	H	6.1283	11.6045	8.0555
H	-2.8711	1.1456	1.8576	H	6.1283	11.6045	8.0555
H	-1.3021	1.2891	1.0726	H	6.1283	11.6045	8.0555
H	-2.2782	2.9160	-0.5957	H	6.1283	11.6045	8.0555
H	-3.8552	2.7727	0.1896	H	6.1283	11.6045	8.0555
H	-1.2948	3.8463	1.5262	H	6.1283	11.6045	8.0555
H	-2.8823	3.7074	2.3171	H	6.1283	11.6045	8.0555
H	-0.6760	10.5651	-4.2897	H	6.1283	11.6045	8.0555
H	-1.4008	11.3416	-2.8682	H	6.1283	11.6045	8.0555
H	-2.3955	10.3186	-3.9254	H	6.1283	11.6045	8.0555
H	-0.0240	9.3166	-2.2134	H	6.1283	11.6045	8.0555
H	-1.0132	8.3014	-3.2628	H	6.1283	11.6045	8.0555
H	-3.0480	8.8372	-1.8557	H	6.1283	11.6045	8.0555
H	-2.0465	9.8494	-0.8044	H	6.1283	11.6045	8.0555
H	-0.6735	7.8617	-0.1592	H	6.1283	11.6045	8.0555
H	-1.6908	6.8237	-1.2153	H	6.1283	11.6045	8.0555
C	8.1127	7.0532	0.5322	H	6.1283	11.6045	8.0555
C	7.2156	7.5708	1.6722	H	6.1283	11.6045	8.0555
C	6.8138	6.4606	2.6686	H	6.1283	11.6045	8.0555
C	5.9031	6.9923	3.7698	H	6.1283	11.6045	8.0555
P	4.3102	5.8705	5.6381	H	6.1283	11.6045	8.0555
O	3.0459	6.1361	4.8826	H	6.1283	11.6045	8.0555
O	5.6355	5.8795	4.7278	H	6.1283	11.6045	8.0555
2. $\text{UO}_2(\text{NO}_3)_2 \text{TiBP}_2$				U	-0.5734	-0.0795	0.1828
				O	-0.0279	1.5223	-0.4659
				O	-1.1186	-1.6873	0.8181

H	2.7995	-4.9016	-1.6425	O	1.4951	3.4456	3.3841
H	1.6405	-4.5444	-2.9381	C	5.0822	2.7475	4.6181
H	1.5533	-6.0997	-2.0756	C	3.7897	3.5045	4.2515
C	-4.9680	-1.9382	-0.6492	C	2.6291	2.5771	3.8611
C	-5.0002	-3.4419	-0.3240	C	2.0636	1.7228	4.9915
C	-3.6249	-4.1175	-0.2566	O	2.2634	4.4166	1.1988
C	-3.6836	-5.5924	0.1356	H	-1.0474	5.4887	-0.4887
P	-1.5508	-3.4493	-1.8756	H	-0.3242	7.0945	-0.2259
O	-1.2567	-2.1225	-1.2485	H	-2.0516	6.9467	-0.5900
O	-3.0221	-4.0348	-1.6356	H	-2.4613	5.7941	1.5983
O	-1.4444	-3.3499	-3.4661	H	-1.7301	7.3799	1.8596
C	-3.5378	-5.4941	-5.8979	H	0.5186	6.2603	2.1433
C	-3.1060	-4.3316	-4.9804	H	-0.0005	5.2426	4.3877
C	-1.6894	-4.4909	-4.4073	H	-1.7308	5.2032	3.9697
C	-0.5700	-4.4212	-5.4442	H	-0.8978	6.7656	4.1642
O	-0.5954	-4.6444	-1.3638	H	4.9539	2.1203	5.5095
H	-4.5213	-1.7547	-1.6330	H	5.8944	3.4566	4.8255
H	-4.3826	-1.3812	0.0931	H	5.4117	2.0985	3.7942
H	-5.9859	-1.5251	-0.6571	H	3.9844	4.1761	3.4056
H	-5.6122	-3.9790	-1.0646	H	3.4681	4.1348	5.0940
H	-5.4803	-3.6009	0.6536	H	2.9246	1.9355	3.0224
H	-2.9681	-3.5618	0.4228	H	1.7144	2.3597	5.8152
H	-2.6830	-6.0383	0.1332	H	2.8395	1.0497	5.3775
H	-4.3195	-6.1527	-0.5626	H	1.2313	1.1095	4.6311
H	-4.1041	-5.6921	1.1450	H	4.1166	6.3866	1.0831
H	-2.9294	-5.5510	-6.8096	U	-0.3435	0.1045	-0.0261
H	-4.5827	-5.3611	-6.2074	O	1.2792	-0.5243	-0.4084
H	-3.4661	-6.4621	-5.3811	O	-1.9601	0.7284	0.3640
H	-3.8022	-4.2555	-4.1366	N	-0.4774	-1.5002	2.8281
H	-3.1536	-3.3775	-5.5246	O	-0.9426	-2.0178	1.7456
H	-1.6158	-5.4224	-3.8313	O	0.0695	-0.3421	2.7237
H	-0.6034	-3.4629	-5.9774	O	-0.5497	-2.0923	3.9169
H	-0.6752	-5.2350	-6.1721	N	-0.4102	1.7794	-2.8309
H	0.4103	-4.5181	-4.9646	O	0.0839	2.2872	-1.7552
H	-0.1688	-6.7775	0.2943	O	-0.8717	0.5861	-2.7453
C	4.2207	6.3854	-0.0092	O	-0.4350	2.4157	-3.8963
C	2.9612	5.8112	-0.6859				
C	2.5693	4.3812	-0.2810				
C	3.6323	3.3139	-0.5335				
H	5.1213	5.8127	-0.2660	C	1.9845	-6.9082	-5.0960
H	4.3863	7.4211	-0.3339	C	1.8772	-5.7471	-4.0906
H	2.1036	6.4674	-0.4858	C	1.3433	-6.1798	-2.7091
H	3.0946	5.8040	-1.7785	C	1.2129	-4.9983	-1.7249
H	1.6463	4.1038	-0.7997	C	0.6806	-5.4324	-0.3631
H	3.8909	3.3036	-1.6010	P	-0.1869	-4.1831	1.8758
H	3.2461	2.3243	-0.2688	O	0.3474	-5.0410	2.9769
H	4.5438	3.5098	0.0444	O	0.5723	-4.2054	0.4741
C	-1.2176	6.4784	-0.0501	O	-1.6981	-4.5468	1.4562
C	-1.5397	6.3763	1.4504	C	-7.7162	-5.8973	2.9836
C	-0.4376	5.7484	2.3142	C	-6.5622	-5.5237	2.0346
C	-0.7845	5.7342	3.8037	C	-5.1929	-5.4355	2.7408
P	1.0912	3.5111	1.8361	C	-4.0473	-5.0584	1.7773
O	0.9092	2.1964	1.1406	C	-2.7080	-4.9083	2.4899
O	-0.2742	4.3397	1.8302	O	-0.1225	-2.6412	2.2938

4. $\text{UO}_2(\text{NO}_3)_2 \cdot \text{TAP}_2$

O	2.7343	2.2447	-1.2787
U	-0.3469	-0.3783	0.1492
O	-0.7683	0.8543	1.4161
O	0.1026	-1.5864	-1.1318
N	-2.5091	-2.2260	1.1498
O	-2.7116	-1.3332	0.2247
O	-1.2925	-2.2474	1.6091
O	-3.3888	-2.9806	1.5524
P	-2.8419	1.2572	-2.4894
O	-1.9491	0.6597	-1.4501
O	-3.0462	2.8392	-2.4372
C	-1.2426	6.2042	-2.2500
C	-2.3557	5.1467	-2.1106
C	-1.8949	3.7746	-2.5884
O	-2.3362	1.0077	-3.9969
C	-0.4433	-1.4032	-6.2809
C	-1.1095	-0.1089	-5.7746
C	-1.6964	-0.2816	-4.3781
O	-4.3202	0.6817	-2.3311
C	-7.8744	0.6189	-3.7157
C	-6.6380	0.2251	-2.8850
C	-5.4431	1.1232	-3.1900
H	-1.5998	7.1810	-1.8995
H	-0.9233	6.3194	-3.2950
H	-0.3594	5.9361	-1.6551
H	-3.2385	5.4491	-2.6917
H	-2.6710	5.0660	-1.0613
H	-1.0572	3.3943	-1.9954
H	-1.6197	3.7794	-3.6495
H	-0.0338	-1.2552	-7.2879
H	-1.1617	-2.2333	-6.3302
H	0.3818	-1.7125	-5.6256
H	-1.9108	0.1984	-6.4620
H	-0.3766	0.7097	-5.7505
H	-0.9296	-0.5198	-3.6350
H	-2.4700	-1.0600	-4.3586
H	-8.1903	1.6497	-3.5023
H	-8.7188	-0.0429	-3.4864
H	-7.6758	0.5454	-4.7943
H	-6.8623	0.2896	-1.8120
H	-6.3591	-0.8179	-3.0879
H	-5.6532	2.1729	-2.9537
H	-5.1347	1.0434	-4.2398
P	2.3268	-1.7435	2.7590
O	1.2809	-1.3950	1.7488
O	3.6471	-2.4514	2.2036
C	6.4610	-2.1832	-0.3703
C	5.5400	-2.7854	0.7097
C	4.4863	-1.7845	1.1692
O	2.9080	-0.4800	3.5693
C	2.0361	2.9561	4.9981
C	2.8706	1.7161	4.6200
C	2.0183	0.6599	3.9266
O	1.7430	-2.8004	3.8009

C	2.4004	-4.8746	6.9357
C	1.6395	-4.2093	5.7731
C	2.5646	-3.3797	4.8887
H	7.2239	-2.9109	-0.6754
H	6.9805	-1.2881	-0.0012
H	5.8928	-1.8950	-1.2648
H	6.1349	-3.1041	1.5774
H	5.0343	-3.6795	0.3195
H	3.8328	-1.4716	0.3489
H	4.9366	-0.8967	1.6282
H	2.6625	3.7032	5.5012
H	1.2130	2.6957	5.6777
H	1.5993	3.4277	4.1074
H	3.3286	1.2792	5.5192
H	3.6908	2.0055	3.9485
H	1.5665	1.0383	3.0059
H	1.2259	0.2842	4.5857
H	3.1829	-5.5545	6.5701
H	1.7125	-5.4614	7.5576
H	2.8805	-4.1275	7.5833
H	1.1494	-4.9712	5.1524
H	0.8441	-3.5585	6.1614
H	3.3459	-3.9945	4.4271
H	3.0338	-2.5605	5.4481

Acknowledgements

R. S. Madyal thanks the Council of Scientific and Industrial Research (CSIR), India, for a Junior Research Fellowship (JRF).

References

- [1] T.H. Siddall, III, *J. Inorg. Nucl. Chem.*, 13 (1960) 151–155.
- [2] S. Nomura and R. Hara, *Anal. Chim. Acta*, 25 (1961) 212–218.
- [3] A. Suresh, T.G. Srinivasan, and P.R. Vasudeva Rao, *Solvent Extr. Ion Exch.*, 12 (1994) 727–744.
- [4] C.V.S. Rao, A. Suresh, T.G. Srinivasan and P.R. Vasudeva Rao, *Solvent Extr. Ion Exch.*, 21 (2003) 221–238.
- [5] C. Sella and D. Bauer, *Solvent Extr. Ion Exch.*, 11 (1993) 395–410.
- [6] C. Sella and D. Bauer, *Solvent Extr. Ion Exch.*, 10 (1992) 579–599.
- [7] C. Sella and D. Bauer, *Solvent Extr. Ion Exch.*, 10 (1992) 491–507.
- [8] C. Rabbe, C. Madic, A. Godard and *Solvent Extr. Ion Exch.*, 16 (1998) 1091–1109.
- [9] A. Varnek, D. Fourches, V.P. Solov'ev, V.E. Baulin, A.N. Turanov, V.K. Karandashev, D. Fara and A.R. Katritzky, *J. Chem. Inf. Comput. Sci.*, 44 (2004) 1365–1382.
- [10] M. Hirata, R. Sekine, J. Onoe, H. Nakamatsu, T. Mukoyama, K. Takeuchi and S. Tachimori, *J. Alloys Comp.*, 271–273 (1998) 128–132.
- [11] Y. Oda, H. Funasaka, Y. Nakamura and H. Adachi, *J. Alloys Comp.*, 255 (1997) 24–30.
- [12] Z.G. Shi and E.A. McCullough, *J. Inclusion Phenom.*, 18 (1994) 9–26.
- [13] A.M. Rozen, B.V. Krupnov and A.A. Bochvar, *Russ. Chem. Rev.*, 65 (1996) 973–1000.
- [14] A.A. Varnek, A.N. Kuznetsov and O.M. Petrukhin, *J. Struct. Chem.*, 30 (1989) 392–396.
- [15] A.A. Varnek, A.N. Kuznetsov and O.M. Petrukhin, *Koord. Khim. Rus.*, 17 (1991) 1038–1041.

- [16] P. Comba, K. Gloe, K. Inoue, T. Krueger, H. Stephan and K. Yoshizuka, *Inorg. Chem.*, 37 (1998) 3310–3315.
- [17] C.D. Auwer, M.C. Charbonnel, M.T. Presson, C. Madic and R. Guillaumont, *Polyhedron*, 13 (1997) 2233–2238.
- [18] J.H. Burns, G.M. Brown and R.R. Ryan, *Acta Cryst.*, C41, 10 (1985) 1446–1448.
- [19] A.K. Rappé, C.J. Casewit, K.S. Colwell, W.A. Goddard and W.M. Skiff, *J. Am. Chem. Soc.*, 114 (1992) 10024–10035.
- [20] A.K. Rappé and W.A. Goddard, *J. Phys. Chem.*, 95 (1991) 3358–3363.
- [21] P.J. Hay, R.R. Martin, L. and G.J. Scheckenbatch, *Phys Chem. A*, 104 (2000) 6259–6270.
- [22] H. Heiberg, O. Gropen, J. Laerdahl, O. Swang and U. Wahlgren, *Theor. Chem. Acc.*, 110 (2003) 118–125.
- [23] A.D. Becke, *Phys. Rev. A*, 38 (1988) 3098–3100.
- [24] C. Lee, W. Yang and R.G. Parr, *Phys. Rev. B*, 37 (1988) 786–789.
- [25] D.D. Koelling and B.N. Harmon, *J. Phys. C: Solid State Phys.*, 10 (1977) 3107–3112.
- [26] M. Douglas and N.M. Kroll, *Ann. Phys. (San Diego)*, 82 (1974) 89–155.
- [27] P. Beudaert, V. Lamare, J.F. Dozol, L. Troxler and G. Wipff, *Solvent Extr. Ion Exch.*, 16 (1998) 597–618.
- [28] L. George, K.S. Viswanathan and S. Singh, *J. Phys. Chem. A*, 101 (1997) 2459–2464.
- [29] L. Troxler, A. Dedieu, F. Hutschka and G. Wipff, *J. Mol. Struct. (Theochem.)* 431 (1998) 151–163.
- [30] P.J. Hay, R.R. Martin, L. and G.J. Scheckenbatch, *J. Chem. Phys.*, 109 (1998) 3875–3881.
- [31] P. Suomalainen, R. Laitinen, S. Jääskeläinen, M. Haukkaa, J. Pursiainen and T. Pakkanen, *J. Mol. Cat. A: Chem.*, 179 (2002) 93–100.
- [32] D. White, *Computational Organometallic Chemistry*, Marcel Dekker, NewYork, 2001, 39 pp.